Inverse design for material anisotropy and its application for a compact X-cut TFLN on-chip wavelength demultiplexer

Jiangbo Lyu[1,2†], Tao Zhu[1,2†], Yan Zhou[1], Zhenmin Chen[1], Yazhi Pi[1], Zhengtong Liu[1], Xiaochuan Xu[2], Ke Xu[2*], Xu Ma[3*], Lei Wang[1*], Zizheng Cao[1*] and Shaohua Yu[1]

[1]Peng Cheng Laboratory, Shenzhen 518055, China; [2]Department of Electronic and Information Engineering, Harbin Institute of Technology (Shenzhen), Shenzhen 518055, China; [3]Key Laboratory of Photoelectronic Imaging Technology and System of Ministry of Education of China, School of Optics and Photonics, Beijing Institute of Technology, Beijing 100081, China.

[†]These authors contributed equally to this work.

*Correspondence: K Xu, E-mail: kxu@hit.edu.cn; X Ma, E-mail: maxu@bit.edu.cn; L Wang, E-mail: wangl07@pcl.ac.cn; ZZ Cao, E-mail: caozzh@pcl.ac.cn

This file includes:

Supplementary information for this paper is available at https://doi.org/10.29026/oes.2023.230038

Section 1: Derivation process of the adjoint method for anisotropic material

For anisotropic materials, the dielectric tensor of the material is given by Eq. (S1):

$$\boldsymbol{\varepsilon} = \begin{bmatrix} \varepsilon_x & & \\ & \varepsilon_y & \\ & & \varepsilon_z \end{bmatrix} . \tag{S1}$$

The bold symbol indicates its matrix form. Nonetheless, the entire system still belongs to a linear system, and the adjoint method can still be used to solve for the gradients of the objective function for each design variable in the optimization region.

Assuming the target function is $\boldsymbol{T}(\boldsymbol{x}(\boldsymbol{p}), \boldsymbol{p})$, and the system adheres to Maxwell equations, succinctly denoted as $\boldsymbol{R}(\boldsymbol{x}(\boldsymbol{p}), \boldsymbol{p}) = 0$, where $\boldsymbol{x}$ represents the electric field and $\boldsymbol{p}$ is normalized permittivity, which signifies the design parameters of the optimization region, the gradients of the target function for the optimization region parameters can be calculated in Eq. (S2)[S1]:

$$\frac{\mathrm{d}\boldsymbol{T}}{\mathrm{d}\boldsymbol{p}_k} = \frac{\partial \boldsymbol{T}}{\partial \boldsymbol{x}}\frac{\mathrm{d}\boldsymbol{x}}{\mathrm{d}\boldsymbol{p}_k} + \frac{\partial \boldsymbol{T}}{\partial \boldsymbol{p}_k} , \tag{S2}$$

where $\boldsymbol{p}_k$ is the normalized permittivity, which represents design parameter.

We observe that within the expression, the most computationally demanding component is $\dfrac{\mathrm{d}\boldsymbol{x}}{\mathrm{d}\boldsymbol{p}}$. If the Finite-Difference Time-Domain (FDTD) method is employed, its expression is denoted as Eq. (S3):

$$\frac{\mathrm{d}\boldsymbol{x}}{\mathrm{d}\boldsymbol{p}} \approx \frac{1}{\Delta\boldsymbol{p}_k}\left(\boldsymbol{x}\left(\boldsymbol{p}_{\Delta p_k}\right) - \boldsymbol{x}(\boldsymbol{p})\right) , \tag{S3}$$

where $\Delta\boldsymbol{p}_k$ is a small change in the kth parameter, and $\boldsymbol{p}_{\Delta p_k}$ is equal to $\boldsymbol{p} + \Delta\boldsymbol{p}_k$.

From this, it is evident that a single computation of $\boldsymbol{R}(\boldsymbol{x}(\boldsymbol{p}), \boldsymbol{p}) = 0$ is required to calculate $\boldsymbol{x}(\boldsymbol{p})$, along with an additional computation of $\boldsymbol{R}\left(\boldsymbol{x}(\boldsymbol{p}), \boldsymbol{p}_{\Delta p_k}\right) = 0$ to determine $\boldsymbol{x}\left(\boldsymbol{p}_{\Delta p_k}\right)$. This implies that two simulations are necessary to obtain the result of a single gradient calculation. For gradients involving n design parameters, $n + 1$ times simulations are required to complete the computation of the full gradients.

However, in the adjoint method, regardless of the number of design parameters $\boldsymbol{p}$, only two simulation computations are required to obtain the complete gradients. The details of the adjoint method are as follows:

Since $\boldsymbol{R} = 0$ is the steady-state solution of the system, the derivative of $\boldsymbol{R}$ with respect to the design parameter $\boldsymbol{p}_k$ is also zero,

$$\frac{\mathrm{d}\boldsymbol{R}}{\mathrm{d}\boldsymbol{p}_k} = \frac{\partial \boldsymbol{R}}{\partial \boldsymbol{x}}\frac{\partial \boldsymbol{x}}{\partial \boldsymbol{p}_k} + \frac{\partial \boldsymbol{R}}{\partial \boldsymbol{p}_k} = 0 . \tag{S4}$$

Hence, the gradients of the target function for the design parameters can be expressed as

$$\frac{\mathrm{d}\boldsymbol{T}}{\mathrm{d}\boldsymbol{p}_k} = \frac{\partial \boldsymbol{T}}{\partial \boldsymbol{x}}\frac{\mathrm{d}\boldsymbol{x}}{d\boldsymbol{p}_k} + \frac{\partial \boldsymbol{T}}{\partial \boldsymbol{p}_k} - \boldsymbol{v}^{\mathrm{T}}\left(\frac{\partial \boldsymbol{R}}{\partial \boldsymbol{x}}\frac{\partial \boldsymbol{x}}{\partial \boldsymbol{p}_k} + \frac{\partial \boldsymbol{R}}{\partial \boldsymbol{p}_k}\right) , \tag{S5}$$

where $\boldsymbol{v}^{\mathrm{T}}$ is adjoint field.

Eq. (S5) can be simplified to Eq. (S6):

$$\frac{\mathrm{d}\boldsymbol{T}}{\mathrm{d}\boldsymbol{p}_k} = \frac{\partial \boldsymbol{T}}{\partial \boldsymbol{p}_k} - \boldsymbol{v}^T\frac{\partial \boldsymbol{R}}{\partial \boldsymbol{p}_k} + \left(\frac{\partial \boldsymbol{T}}{\partial \boldsymbol{x}} - \boldsymbol{v}^T\frac{\partial \boldsymbol{R}}{\partial \boldsymbol{x}}\right)\frac{\partial \boldsymbol{x}}{\partial \boldsymbol{p}_k} . \tag{S6}$$

As can be seen from Eq. (S6), it is only necessary to find a variable v that satisfies Eq. (S7):

$$\left(\frac{\partial \boldsymbol{T}}{\partial \boldsymbol{x}} - \boldsymbol{v}^{\mathrm{T}}\frac{\partial \boldsymbol{R}}{\partial \boldsymbol{x}}\right)\frac{\partial \boldsymbol{x}}{\partial \boldsymbol{p}_k} = 0 . \tag{S7}$$

This allows for the elimination of the $\dfrac{\partial \boldsymbol{x}}{\partial \boldsymbol{p}_k}$ term, enabling the complete gradients to be obtained through two simulation computations.

Therefore, the equations for the two simulation processes of the adjoint method, derived from Maxwell equations and the material equation $\boldsymbol{D} = \boldsymbol{\varepsilon}\boldsymbol{E}$, are as follows:

$$Ax = b \,, \tag{S8}$$

$$A^{\mathrm{T}}v = \left(\frac{\partial F}{\partial x}\right)^{\mathrm{T}} \,, \tag{S9}$$

where A is Maxwell operator, denoted specifically as $A = \begin{bmatrix} \varepsilon \ (-t)^{\mathrm{T}} * \partial_t & \nabla \times \\ \nabla \times & -\mu\partial_t \end{bmatrix}$. It is important to note that the variables in bold in the equations are in matrix form.

Section 2: Wavelength division demultiplexer with 25 µm×10 µm footprint

A 25 µm ×10 µm thin film lithium niobate (TFLN) wavelength division demultiplexer is obtained using the scalar-based inverse design method and works in the spectral range of 1510–1580 nm. By default, Z-cut TFLN material is used, as such the scalar-based isotropic inverse design method can be readily applied. A schematic of the obtained device structure is shown in Fig. S1. On the left is the input port of the broadband signal, and on the right are the four output ports. Ports 1, 2, 3, and 4 correspond to the wavelength ranges of 1510–1520 nm, 1530–1540 nm, 1550–1560 nm, and 1570–1580 nm, respectively. Each port has a designed spectral width of 10 nm. Between each pair of neighboring ports, there is a 10 nm isolation in the wavelength spectrum and a physical spacing of 2.5 µm between adjacent waveguide ports. In the initialization, the design area size is set to 25 µm × 10 µm. A slab waveguide is placed in the 25 µm × 10 µm design region with a thickness of 250 nm as the initial structure to transmit light waves from the input end to the output ends. The mesh size is set to 50 nm and the minimum feature size is set to 200 nm.

In the scalar-based inverse design process, the targeted values of refractive index in the design area are optimized between the waveguide refractive index and the cladding refractive index and eventually binarized. We first set the upper and lower limiting refractive index values to 2.21 and 1.44, respectively. We then set the target transmittance of the TE mode optical signal as 1 for each port.

Design region: 25 µm×10 µm

2.5 µm

Scalar-based isotropic
inverse design

▢ X-cut LN
▢ Background
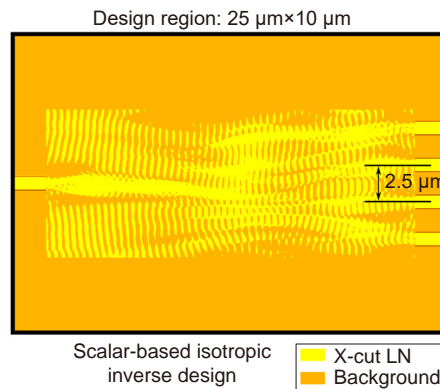
Fig. S1 | (a) Schematic of a TFLN four-port wavelength division demultiplexer obtained using the scalar-based inverse design method with 25 µm × 10 µm footprint.

For the default structure, spectral response from four output ports is shown in Fig. S2(a) to serve as a benchmark. The spectral response of the same structure after setting the material to the tensor form of X-cut TFLN is shown in Fig. S2(b). Results show that the traditional scalar-based inverse design method is not suitable for anisotropic materials (X-cut TFLN). The performance of the X-cut TFLN device designed by our proposed inverse design method (Fig. 6) is comparable to that of the Z-cut TFLN device obtained by classical method.
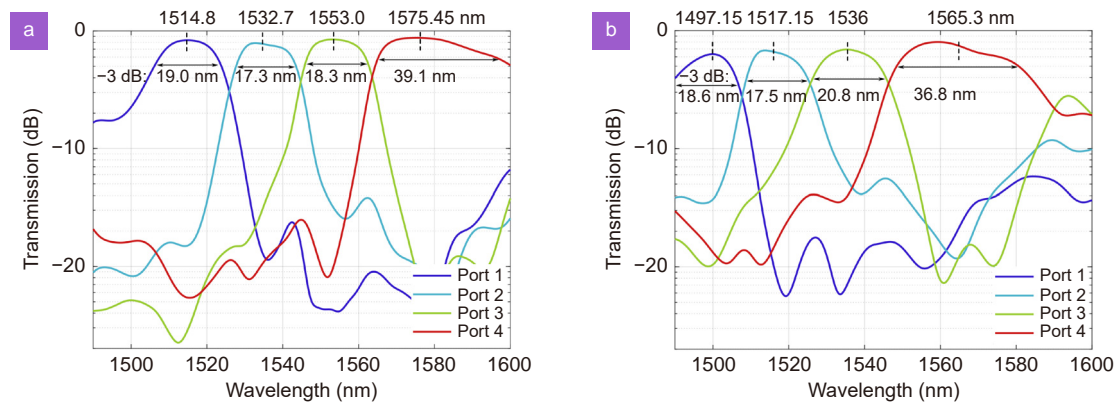
Fig. S2 | (a) Spectral response of Z-cut TFLN wavelength division demultiplexer obtained by the scalar-based inverse design method. **(b)** Spectral response of the same structure after setting the material to the tensor form of X-cut TFLN.

Section 3: Intermediate results during optimization

During optimization process (Fig. S3), the FOM of port 2 and port 3 drop quickly while FOM of 1 and 4 stays the same. After some iteration, the FOM of 1 and 4 starts to drops.
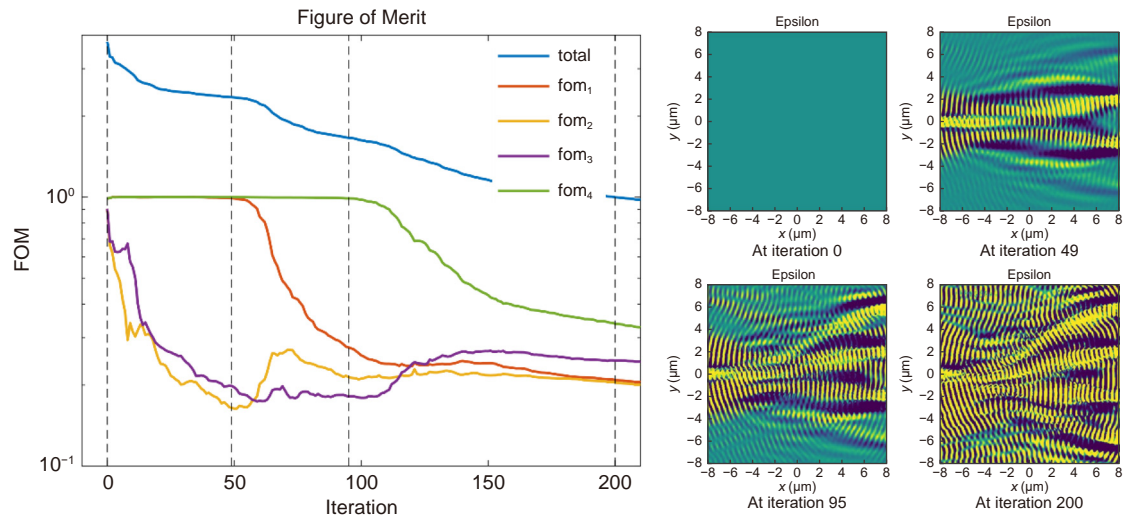
Fig. S3 | Four intermediate results during the optimization of a 16 μm ×16 μm wavelength division demultiplexer at iteration 0, iteration 49, iteration 95 and iteration 200, respectively.

Here is the explanation for this phenomenon:

This phenomenon is related to the adjoint method, which is widely recognized as a classical approach for conserving computational resources. When calculating the gradients of objective function with respect to the design variables, all gradients within the optimization region can be obtained through two simulations: a forward simulation and an adjoint simulation.

In the forward simulation, the light enters waveguide and the mode overlap integral is calculated at the output waveguide. After completing the forward simulation, based on its results, an adjoint light source is generated at the output waveguide, and the adjoint simulation is conducted. As mentioned above, in the adjoint simulation, the light propagates in the reverse direction, which requires to solve the solution of the adjoint field to reduce computational demand and to compute the complete gradients of objective function with respect to the design variables. However, in the adjoint simulation, the value of the adjoint sources is related to E field of monitors in forward simulation. The different values of the adjoint sources lead to a different optimization order of these ports.

Given that the initial structure is a planar waveguide, it is foreseeable that the adjoint sources generated at ports 2 and 3 will be larger than those at the other two ports. This leads to ports 2 and 3 being the first to be optimized during the optimization process. In subsequent iterations, the transmittances of ports 2 and 3 will gradually increase. When the

changes of the design parameters cannot enhance the performance of ports 2 and 3 anymore, ports 1 and 4 begin to be optimized, and the adjoint source terms for these ports also gradually increase. This process continues until the algorithm converges to a local optimum, at which point the iteration is terminated.

Here, we take the optimization process of 16 μm × 16 μm wavelength division demultiplexer based on scalar-based inverse design method as an example. In Fig. S3, we show four intermediate results during the optimization at iteration 0, iteration 49, iteration 95 and iteration 200, respectively. At the beginning of optimization, the design region is a planar waveguide, so the value of epsilon is uniform, and the light is freely transmitted within the region. At iteration 49, the shape of the waveguides route to port 2 and port 3 can be seen from the epsilon distribution map, while the waveguides route to port 1 and 4 have not yet started to be optimized. After iteration 60, the waveguide route to port 1 started to be optimized. After iteration 100, the waveguide route to port 4 started to be optimized. At iteration 200, the prototype of the final design device can be seen from the epsilon distribution map.

References

S1. Niederberger ACR, Fattal DA, Gauger NR, Fan SH, Beausoleil RG. Sensitivity analysis and optimization of sub-wavelength optical gratings using adjoints. *Opt Express* **22**, 12971–12981 (2014).